The AAPS Journal, Vol. 15, No. 1, January 2013 (© 2012)
DOI: 10.1208/s12248-012-9418-6

Research Article

Biodegradable Particles as Vaccine Delivery Systems: Size Matters

Vijaya B. Joshi,[1] Sean M. Geary,[1] and Aliasger K. Salem[1,2]

Received 27 June 2012; accepted 24 September 2012; published online 10 October 2012

Abstract. Poly(lactide-co-glycolide) (PLGA) particles have strong potential as antigen delivery systems. The size of PLGA particles used to vaccinate mice can affect the magnitude of the antigen-specific immune response stimulated. In this study, we fabricated and characterized 17 μm, 7 μm, 1 μm, and 300 nm PLGA particles coloaded with a model antigen ovalbumin (OVA) and CpG oligodeoxynucleotides (CpG ODN). PLGA particles demonstrated a size-dependent burst release followed by a more sustained release of encapsulated molecules. PLGA particles that were 300 nm in size showed the highest internalization by, and maximum activation of, dendritic cells. The systemic antigen-specific immune response to vaccination was measured after administration of two intraperitoneal injections, 7 days apart, of 100 μg OVA and 50 μg CpG ODN in C57BL/6 mice. *In vivo* studies showed that 300 nm sized PLGA particles generated the highest antigen-specific cytotoxic T cell responses by days 14 and 21. These mice also showed the highest IgG2a:IgG1 ratio of OVA-specific antibodies on day 28. This study suggests that the smaller the PLGA particle used to deliver antigen and adjuvants the stronger the antigen-specific cytotoxic T cell response generated.

KEY WORDS: CpG ODN; cytotoxic T lymphocytes; dendritic cells; nanoparticles; poly (lactide-co-glycolide); vaccine.

INTRODUCTION

The worldwide prevalence of malignant and intracellular pathogenic diseases necessitates the development of novel prophylactic and therapeutic vaccine strategies. A major consideration for treatment of many diseases is that such vaccines should stimulate a cellular adaptive immune response which involves generation of cytotoxic T lymphocytes (CTLs) capable of recognizing pathogen-associated antigens (Ags). These Ag are endogenously expressed by infected cells in association with MHC class I surface molecules (1). Vaccines to intracellular diseases need to trigger the activation of dendritic cells (DCs) in a fashion that maximizes CTL activation.

When DCs are activated, they can stimulate either Th1-type or Th2-type biased immune responses. Stimulation of Ag-specific CTL tends to be correlated with Th1-type responses. Whether a vaccine generates a primarily Th1-type or Th2-type immune response is largely dependent on the properties of that vaccine (2–4).

It has become increasingly evident that in order to generate a Th1-type response, the Ag should be delivered to DC in a particulated form (5–7). Delivering Ag in particles seems to be important for at least four main reasons: (a) Particles are thought to mimic pathogens and are thus readily phagocytosed by DC (8,9). (b) Particles can protect encapsulated Ags from degradation by systemic proteases prior to being phagocytosed (10). (c) Particles can be coloaded with multiple molecules. (d) Particulated Ags show a greater degree of cross-presentation by DCs as compared to soluble Ags (11).

A number of studies have shown that vaccines carrying Ag alone is not sufficient to stimulate robust CTL activity (12). CpG oligodeoxynucleotides (CpG ODN) stimulate a Th1 biased response through the intracellular Toll-like receptor 9 (TLR9). Biodegradable particles are effectively internalized by DCs and macrophages and are therefore ideal for delivering CpG ODN to its target site thereby enhancing the Th1 response to an Ag also encapsulated in the microparticle. We have previously shown that microparticles entrapping both a model Ag, ovalbumin (OVA), and CpG ODN induced significantly higher amounts of anti-OVA antibody production than soluble OVA and CpG ODN, and stimulated stronger IgG2a production than microparticles entrapping Ag alone. While the presence of CpG ODN in the microparticles did not impact on the phenotype of the DCs, it was necessary for DCs to induce activation of Ag-specific T cells as inferred by interferon gamma (IFN-γ) production (10).

A wide range of viral and nonviral particulated vaccine delivery systems have been reported in the literature showing optimum activation of DCs and/or T cell proliferation (8,13–16). Poly(lactide-co-glycolide) (PLGA)-based delivery systems are nontoxic biodegradable delivery vehicles (17) which can provide sustained delivery of Ag

[1] Department of Pharmaceutical Sciences and Experimental Therapeutics, College of Pharmacy, University of Iowa, Iowa City, Iowa 52242, USA.
[2] To whom correspondence should be addressed. (e-mail: aliasger-salem@uiowa.edu)

and are an attractive approach to stimulating Ag-specific immune responses. However, there are some discrepancies in the literature with respect to the optimum delivery system needed to stimulate adaptive immunity. The charge, shape, and site of delivery of particles can considerably affect the extent of particle uptake and immune stimulation (18–20). It is also critical to identify the optimal size of particles for codelivery of Ag and adjuvants. Some studies have shown that micron-sized particles provide a longer duration of release of Ag resulting in enhanced Ag presentation by DCs (16,21–23). One study found that 2–8 μm sized Ag-encapsulated PLA particles resulted in higher antibody titers than 200 or 400 nm particles. However, this same study also showed that immunization with 200 – 600 nm nanoparticles was associated with higher levels of IFN-γ production, upregulation of MHC class I molecules, and production of antibody isotypes favoring Th1-type immune responses. Immunization with 2 – 8 μm microparticles promoted IL-4 secretion, upregulated MHC class II molecules, and favored Th2-type immune responses (24). In addition, microparticles are more difficult to internalize than nanoparticles. Some studies have argued that Ag delivery systems should mimic viruses or bacteria for effective stimulation of DCs and have shown that nanoparticles generate a high number of activated DCs (25) and stronger CTL responses (13,14,26). Drawbacks to nanosized polymer particles are that they can release the loaded Ag before reaching DC, have lower Ag and adjuvant loading efficiencies than larger particles, and thus coloading Ags and adjuvants is more challenging (27).

To our knowledge, this is the first study to correlate the size of Ag/adjuvant-loaded PLGA-based particulated vaccines with the magnitude of the *in vivo* generated CTL response. Identification of optimal sized particles would help in the fabrication of vaccines with an adequate balance of immunogenicity and delivery capacity to ultimately generate robust Ag-specific immune responses.

In this study, we have coloaded a model Ag, OVA, with CpG ODN in differently sized PLGA particles. We identify a relationship between the size of PLGA particles and the magnitude of the *in vivo* Ag-specific CTL response stimulated. PLGA particles have been reported to improve Ag delivery to DC (6). They are stable during storage and have been shown to protect loaded molecules (28) making it a promising delivery system for adjuvants and antigen. We found that 300 nm particles were the most efficient at Ag and adjuvant delivery to DCs and induced the greatest Ag-specific CTL responses compared to all experimental size groups tested. Our results suggest that the smaller the size of the PLGA particles used the more effective they will be as vaccine delivery systems for treatment and protection against a wide range of infectious diseases.

MATERIALS AND METHODS

Model Antigen OVA and Adjuvant CpG ODN

In this study, we have used OVA, the albumin protein from chicken egg white as a model Ag because it has been well characterized in the literature making comparisons to previous findings more amenable. We have co-administered CpG ODN with OVA. CpG ODN are comprised of an unmethylated phosphodiester backbone of cytosine and guanine dinucleotide sequence 5′-TCCATGACGTTCCTGACGTT-3′ and it mimics the immunostimulatory effects of bacterial DNA (29). CpG ODN is a very potent stimulator of DCs (30) which, as described above, initiate CTL responses. CpG ODN has also shown strong activation for NK cells and B lymphocytes (31) which secrete specific cytokines to enhance T cell proliferation leading to further enhancements in CTL activity.

Fabrication and Characterization of Different Sizes of PLGA Particles Loaded with CpG ODN and OVA

Particles were prepared using the double emulsion solvent evaporation method followed by differential centrifugation to separate groups of different sizes of particles. For preparation of particles, 2 mg of OVA (Sigma, St Louis, MO, USA) and 1.5 mg of CpG ODN (Integrated DNA Technologies, Coralville, IA, USA) were dissolved in 100 μl of 1% poly(vinyl alcohol) (PVA; Mowiol® 8–88; MW: ~67000; Sigma, Allentown, PA, USA) solution making a $water_1$ phase. Two hundred milligrams of PLGA (Resomer® RG 503; viscosity: 0.32–0.44 dl/g; MW: 24,000–38,000; Boehringer Ingelheim KG, Germany) was dissolved in 1.5 mL of dichloromethane (DCM) to create the oil phase. A primary emulsion was prepared by sonication of the $water_1$ phase into the oil phase for 30 s using a sonic dismembrator (Model 100 equipped with an ultrasonic converter probe; Fisher Scientific, Pittsburgh, PA, USA) at 10 W which was then emulsified into a 1% aqueous PVA solution using two different methods.

In method1, the primary emulsion was homogenized for 30 s in 30 mL of 1% PVA solution using an Ultra-Turrax homogenizer (T 25 basic with 12.7 mm rotor; IKA-werke; Wilmington, NC, USA) at 13,500 rpm/min. In method 2, the primary emulsion was emulsified into 8 mL of 1% PVA solution for 30 s using the sonic dismembrator at 10 W. This secondary emulsion was added to 22 mL of 1% PVA. Secondary emulsions were stirred in a fume hood to allow DCM to evaporate.

Particles were then sequentially centrifuged at 200 rpm (7 × *g*), 1,000 rpm (164 × *g*), 4,000 rpm (2,880 × *g*), and 7,000 rpm (6,790 × *g*) for 5 min using Eppendorf centrifuge 5804 R (Eppendorf, Westbury, NY, USA). Pellets obtained at each speed were washed separately with distilled water followed by freeze drying using FreeZone 4.5 (Labconco Corporation, Kansas City, MO, USA). Alternative particle size separation methods such as the Ficoll gradient column method were also evaluated and found to be inappropriate for these studies because of residual sugar from the high sucrose content needed for the separation.

The encapsulation efficiency of the fabrication process was calculated as described in Eq. 1. To estimate loading of OVA and CpG ODN, 20 mg of particles from each batch were incubated with 0.2 N NaOH for 12 h. Once a

clear solution was obtained, it was neutralized using 1 N HCl and loading was calculated using Eq. 2.

$$\text{Encapsulation efficiency} = [(\text{weight of PLGA particles} \times \text{loading of OVA or CpG})/\text{total amount of OVA or CpG}] \times 100 \quad (1)$$

$$\text{Loading capacity} = \left(\begin{array}{l} \text{concentration of OVA in neutralized solution of NaOH} \\ \times \text{Volume of neutralized solution containing degraded particles} \end{array} \right) / \text{weight of degraded particles} \quad (2)$$

Scanning Electron Microscopy

The surface morphology and shape of PLGA particles was examined using scanning electron microscopy (SEM). Briefly, a suspension of particles was plated on a silicon wafer mounted on a SEM stub. Wafers were coated with gold–palladium by an argon beam K550 sputter coater (Emitech Ltd., Kent, England). Images were captured using the Hitachi S-4800 SEM (Hitachi High-Technologies, Ontario, Canada) at 5 kV accelerating voltage. The average sizes of particles were calculated using ImageJ software (US National Institutes of Health, Maryland, USA) with n=100.

Estimation of *In Vitro* Release of OVA and CpG ODN from PLGA Particles

Fifty milligrams of particles were added to 3 mL of phosphate buffered saline (PBS) at pH 7.4 and incubated in a 37°C incubator shaker running at 200 rpm/min. At predetermined time intervals, 500 μL of supernatant was removed after centrifugation at 6,800 × g for 5 min and replaced with fresh PBS equilibrated to 37°C. Quantification of OVA in supernatant samples was performed using a standard Micro BCA™ assay kit (Pierce Chemical Co. Rockford, IL, USA) at 562 nm absorbance. CpG-ODN was quantified using fluorescence OliGreen® assay kit (Molecular Probes, Eugene, OR, USA) with excitation at 480 nm and emission at 520 nm. Absorbance and fluorescence intensities were measured using SpectraMax® M5 multimode microplate reader (Molecular Devices, Sunnyvale, CA, USA).

Confocal Microscopy to Study Uptake of PLGA Particles

JAWS II cells (ATCC CRL-11904), an immature DC cell line derived from C57BL/6 bone marrow, were maintained in complete alpha MEM medium containing 20% FBS, 5 ng/ml of GM-CSF, and antibiotics. Rhodamine B loaded particles were prepared using the method described above, except OVA and CpG were replaced by 5 mg of Rhodamine B (Sigma, St Louis, MO, USA). Then 10^4 cells were incubated with 1 μg of Rhodamine B-loaded PLGA particles for 24 h at 37°C. Cells were then washed and fixed using 4% glutaraldehyde followed by staining of nuclei using DAPI. Images were acquired using Zeiss 710 confocal microscope (Carl Zeiss Microscopy, Thornwood, NY, USA).

Using Flow Cytometry to Quantify Uptake of PLGA Particles

JAWS II cells were treated with PLGA particles loaded with Alexa Fluor® 488 conjugated OVA (AF488-OVA) and evaluated by flow cytometry to compare the amount of Ag delivered to the cells by differently sized particles. AF488-OVA was prepared using a Alexa Fluor® 488 succinimidyl ester kit (Invitrogen Life Technologies, Grand Island, NY, USA). Briefly, 10^4 JAWS II cells were incubated at 37°C for 24 h with 1 μg of AF488-OVA loaded in different sizes of PLGA particles. Cells were then washed and incubated with propidium iodide to stain dead cells. Samples were then acquired on the Becton Dickinson FACScan™ with BD CellQuest Pro software and then analyzed using the FlowJo analysis package (Tree star, Standford).

Assessment of Activation of Bone Marrow-Derived Dendritic Cells (BMDCs)

Preparation and Culture of BMDCs

Male C57BL/6 mice were euthanized according to University of Iowa Institutional Animal Care and Use Committee guidelines. BMDCs were prepared using a protocol described by Lutz *et al.* (32). Briefly, mice were sacrificed using a carbon dioxide chamber method followed by cervical dislocation. Femur and tibia were isolated from the legs and bone marrow was flushed using a 30-gauge needle. Cells were grown for 10 days in 20 ng/mL of granulocyte macrophage colony-stimulating factor (GM-CSF).

Flow Cytometry to Quantify the Expression of CD86 and MHC Class I Molecules of BMDCs

Antigen-specific CTLs are generated when Ag is appropriately presented by activated DCs. This presentation is achieved *via* dual signals from the Ag presented in MHC class I molecules and the costimulatory signal of CD86. Thus, relative expression of these surface molecules in treated DCs serve as activation markers of DCs. To estimate the upregulation of these surface molecules, 10^5 BMDCs were incubated with 4 μg of OVA and 2 μg of CpG ODN loaded in

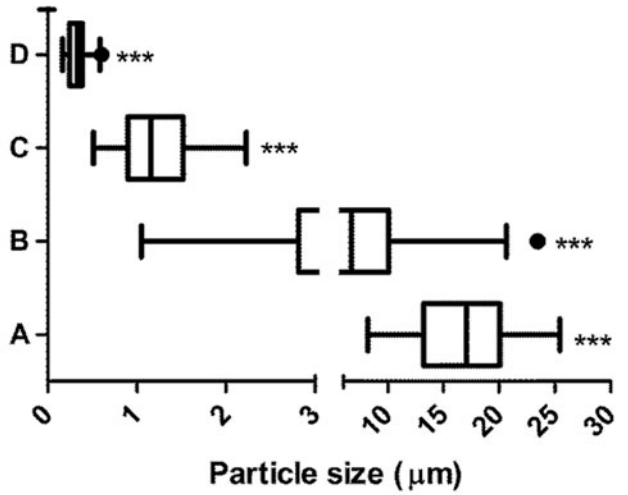

Group	Sizes (Mean ± SD) (μm)	Median size (μm)
A	15.9 ± 3.7	17.4
B	5.5 ± 3.8	6.7
C	1.1 ± 0.3	1.2
D	0.3 ± 0.1	0.3

Fig. 1. Box plot of size distribution of different groups of particles as determined using scanning electron microscopy (SEM) images (n=4) analyzed by Image J software. Each *box* represents the first quartile, median, and third quartile of the size distribution with whiskers representing 1.5 times the interquartile distance. Particles collected at *A* 7×*g*, *B* 164×*g*, *C* 2,880×*g*, *D* 6,790×*g* show significantly distinct distributions in size as analyzed by Kruskal–Wallis one-way analysis of variance followed by Dunns post-test analysis. Group B showed the highest polydispersity with a substantial tail of larger sized particles. ***$p<0.001$. The table enumerates the mean and median size of different groups of PLGA particles

different sizes of PLGA particles for 48 h at 37°C. To analyze the cells by flow cytometry, the cells were flushed, washed, and resuspended in FACS buffer (1% v/v BSA and 0.02% azide in PBS). Cells were stained with PE rat anti-mouse CD86 (BD Biosciences, San Diego, CA, USA) and FITC antimouse MHC class I (eBiosciences, San Diego, CA, USA) monoclonal antibodies at a final concentration of 5 μg/mL. Following staining, cells were washed with FACS buffer and fixed with 4% paraformaldehyde in PBS. Samples were acquired on the FACScan flow cytometer and analyzed using the FlowJo analysis package.

Table I. Influence of the Secondary Emulsification Process on the Size of PLGA Particles (n=3)

	Method 1	Method 2
17 μm[a]	39.2±0.6	0.0
7 μm[a]	60.8±0.6	13.4±1.2
1 μm[a]	0.0	63.2±1.5
300 nm[a]	0.0	23.4±2.7
Percentage recovery[b]	89.8±5.1	75.5±5.3

Secondary emulsion was prepared using homogenization in method1 and sonication in method2

[a] Weight percent from the total weight of recovered particles

[b] Weight percentage of polymer particles recovered with respect to starting material

Table II. Loading of OVA and CpG ODN in Different Sizes of PLGA Particles (n=3)

Group name	OVA (μg/mg PLGA particles)	CpG ODN (μg/mg PLGA particles)
17 μm	7.4±1.3	4.8±0.4
7 μm	8.1±0.7	4.5±0.2
1 μm	7.6±0.2	3.2±0.3
300 nm	5.7±0.7	2.4±0.4

Immunization of Mice with Different Sizes of PLGA Particles

Four groups of male C57BL/6 mice (n=4) were treated with OVA and CpG ODN-loaded PLGA particles with a median size of (a) 17 μm, (b) 7 μm, (c) 1 μm, and (d) 300 nm. Two additional control groups of mice were treated with either (e) soluble OVA and CpG ODN or were (f) naïve. Each mouse was primed on day 0 and boosted on day 7 with an intraperitoneal injection of an equivalent dose of 100 μg of OVA and 50 μg of CpG ODN. Frequencies of OVA specific cytotoxic T cells in blood were measured on days 14 and 21 using tetramer staining and OVA specific IgG antibodies were measured on day 28 using an enzyme-linked immunosorbent assay (ELISA).

Estimation of OVA Specific Cytotoxic T Cell Frequencies in Peripheral Blood

To estimate the proportion of OVA-specific cytotoxic T cells, peripheral blood lymphocytes (PBLs) were stained with H2-Kb SIINFEKL Class I iTAgTM MHC Tetramer (Kb-OVA257; Beckman Coulter, Fullerton, CA, USA). PBLs were also double stained with FITC rat anti-mouse CD8 (eBioscience, San Diego, CA, USA) and PE-Cy5 hamster anti-mouse CD3 (eBioscience, San Diego, CA, USA) monoclonal antibodies which allow T cells to be differentiated from the rest of the lymphocyte population (33).

Briefly, PBLs were obtained by submandibular bleeding and red blood cells were lysed using ammonium chloride potassium buffer (NH_4Cl 8.29 g/L; $KHCO_3$ 1.00 g/L; disodium EDTA·$2H_2O$ 0.0372 g/L in cell culture grade water). Lymphocytes were collected at 220 × *g* and stained with anti-CD8, anti-CD3, and Kb-OVA257. These cells were then washed and fixed with BD Cytofix™ (4% paraformaldehyde in PBS; BD Biosciences, San Diego, CA, USA). Samples were then acquired using a FACScan flow cytometer.

Estimation of Anti-OVA Antibodies in Peripheral Blood Using the Enzyme-Linked Immunosorbent Assay

Delivery of Ag and adjuvant induces mixed IgG subtype antibody responses that can have a significant effect on treatment or prevention of disease (2,3). Higher proportions of IgG2a antibodies relative to IgG1 antibodies correlate with secretion of a set of cytokines that favor CTL proliferation (4). Thus, a higher IgG2a:IgG1 is desirable to generate an Ag specific cellular response as a result of vaccination (34). To estimate levels of these antibodies in peripheral blood, serum samples were collected *via*

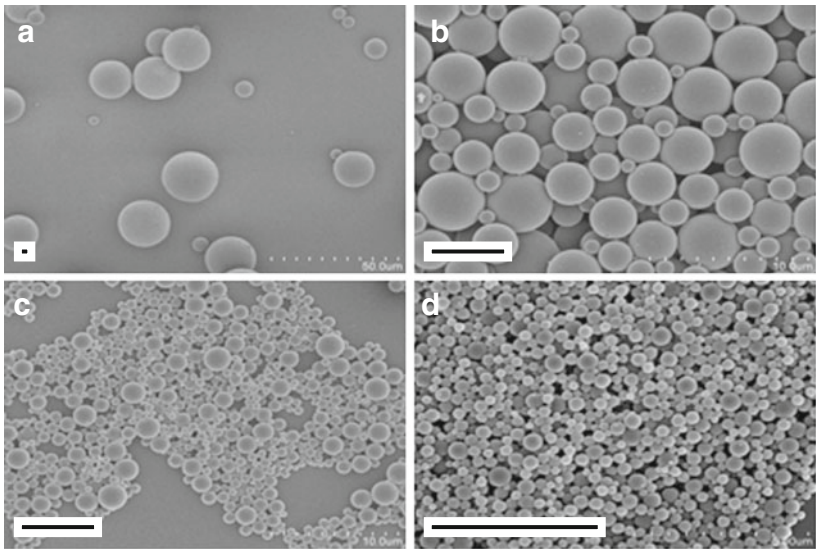

Fig. 2. Scanning electron microscopy (SEM) images of each group of PLGA particles loaded with OVA and CpG-ODN showing smooth morphology and distinct size distributions. The *rectangle* on the bottom left of each image represents a 5 μm scale bar

submandibular bleeding. Serial dilutions of the serum samples were then incubated on ELISA microwell plates (Corning, Lowell, MA, USA) that had been previously coated with 5 μg/mL of OVA solution in PBS. Plates were then washed with PBS-tween, followed by incubation with alkaline phosphatase conjugated goat anti-mouse IgG antibodies (Southern Biotech, Birmingham, AL, USA). Excess antibody was then washed followed by addition of *p*-nitrophenylphosphate in the dark. Absorbance was measured after 2 h at 405 nm using SpectraMax® Plus384 microplate reader.

Statistical Analysis

All experiments were repeated at least in triplicate. Groups for nonparametric analysis were compared by Kruskal–Wallis one-way analysis of variance followed by Dunn's post-test analysis comparing all pairs of treatments. For parametric tests, groups were compared by one-way analysis of variance followed by Tukey's post-test to compare all pairs of treatments. Differences were considered significant at *p*-values that were less than or equal to 0.05.

RESULTS AND DISCUSSION

Preparation and Characterization of Different-Sized PLGA Particles Coloaded with OVA and CpG ODN

Polydispersed PLGA particles prepared from a double emulsion solvent evaporation process (10) were segregated into four size ranges of PLGA particles (A, B, C, and D) by differential centrifugation at 7 × *g*, 164 × *g*, 2,880 × *g*, and 6,790×*g*, respectively. The box plots in Fig. 1 show the median, first, and third quartile of the size distribution of all four batches which were found to be significantly different ($p<0.001$) from each other. Particles of group D and C are nanoparticles and microparticles, respectively, with narrow size ranges. In group B, 50% of particles are within the range of 2.9 – 9 μm which are easily phagocytosed by APCs whereas in group A, 50% of particles are within the range of 13 – 20 μm which are difficult to be phagocytosed by APCs. The sizes and polydispersity of particles in groups D and C were also verified using dynamic light scattering (Zetasizer Nano ZS, Malvern) to ensure the validity of the approach used to measure particle sizes across groups A to D.

These size ranges were selected to delineate the effect of different sizes of PLGA particles in producing an *in vivo* Ag-specific immune response. Figure 1 displays the mean and median size of the four different batches of the particles.

In order to generate the required range of particle sizes, two methods were used where the secondary emulsions were prepared by homogenization and sonication in methods 1 and 2, respectively. Method 1 resulted in particles with a median size of 17 and 7 μm. While method 2 resulted in a higher percentage of smaller-sized particles predominantly with median size ranges of 300 nm and 1 μm as described in Table I. Encapsulation efficiency of OVA was 37.7 (sd: 0.3)% and 38.0 (sd: 1.6)% with methods 1 and 2, respectively. Encapsulation efficiency of CpG was 30.2 (sd: 2.0)% with method1 and 21.9 (sd: 1.8)% with method2. Antigen loading of groups of particles is presented in Table II. In this study, each batch of particles is referred to by its median size. Each batch of particles had distinct size distributions and had smooth and spherical morphologies as shown in Fig. 2.

Percentage Release of OVA and CpG ODN is Dependent on the Size of PLGA Particles

All sizes of PLGA particles show a burst release of encapsulated molecules. However, the extent of burst release decreases with increasing particle size. Figure 3 describes the percentage release of OVA ((i) in Fig. 3) and CpG ODN ((ii) in Fig. 3) at different time points showing that the release of encapsulated molecules was governed by the size of PLGA particles. Particles of 300 nm in size released most of its loaded Ag in approximately 48 h. This can be attributed to lower loading and larger surface area to volume ratio of 300 nm PLGA particles relative to larger sized particles. All other particle groups demonstrated a size dependent

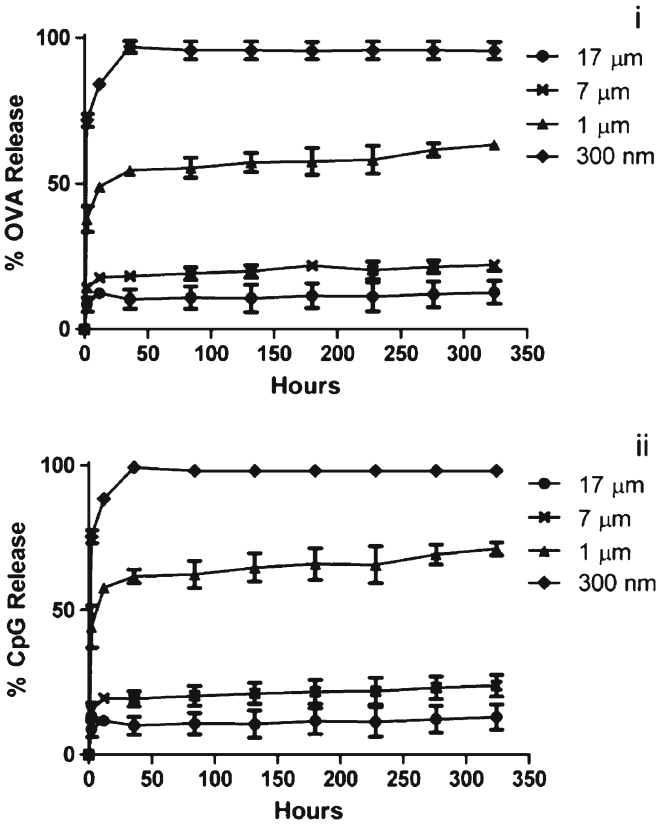

Fig. 3. (*i*) OVA and (*ii*) CpG ODN release in PBS (pH7.4) at 37°C from OVA and CpG ODN co-loaded PLGA particles of different sizes. All the PLGA particles demonstrated burst release. The extent of burst release was dependent on the size of the particles with smaller particles giving larger burst releases

sustained release profile after the burst release with larger particles retaining Ag for longer periods of time than smaller particles. It should be noted that the release studies were performed in PBS at 37°C. The presence of enzymes and serum could modify these release profiles *in vivo*.

Size-Dependent Uptake of PLGA Particles in a Dendritic Cell Line

Uptake of different-sized rhodamine-loaded PLGA particles by dendritic (JAWS II) cells was studied using confocal microscopy (Ziess-710). Confocal microscopy images (n=10) showed that cells had significant uptake of 300 nm sized particles. Particles of 7 and 1 μm sizes were also internalized by JAWS II although to a lesser extent. The large size of 17 μm particles resulted in very low uptake by the JAWS II cells. Figure 4 shows representative images from each treatment group. Interestingly, particles of 300 nm were found in the cytoplasm as well as the nucleus of DCs. This phenomenon is consistent with previous observations by us and others (35,36). PLGA particle uptake increased as the size of the particle decreased.

Efficiency of Uptake of PLGA Particles is Dependent on Size

Flow cytometric analysis of JAWS II cells incubated with AF488-OVA loaded particles gave an insight in to the degree of Ag delivery efficiency by different sizes of particles. Particulated OVA demonstrated a higher uptake of AF488-OVA by DCs as compared to nonparticulated AF488-OVA treatment which is in agreement with previous studies (11,37). Compared to other treatment groups, PLGA particles of sizes 7 μm, 1 μm, and 300 nm were significantly more efficient (p<0.001) in delivering AF488-OVA to JAWS II cells ((i) in Fig. 5). The significant shift of median fluorescence intensity shows that the size of PLGA particles can be correlated to Ag delivery efficiency. PLGA particles that were 300 nm in size generated the maximum intracellular delivery of antigens. Representative histograms showing the relative fluorescence shift of the live cells treated with different sizes of particulated and nonparticulated AF488-OVA is displayed in Fig. 5 (ii).

Particle-Mediated Activation of BMDC is Size Dependent

DCs show enhanced surface expression of MHC and CD80/CD86 co-stimulatory molecules upon activation (38). To understand the effect of particle size on stimulating BMDCs, we studied the relative surface expression of CD86 and MHC class I molecules in BMDCs after treating them with different sizes of PLGA particles carrying 4 μg of OVA and 2 μg of CpG. We found that after 48 h treatment, 300 nm sized particles generated the highest fraction of activated BMDCs as shown in Fig. 6. We hypothesize that the high uptake of smaller particles in combination with quick release of CpG is the reason for the higher number of activated DCs observed in this group. Particle sizes of 7 and 1 μm, and soluble Ag also caused a significant increase (p<0.001) in the fraction of stimulated BMDCs when compared with untreated populations. In contrast, BMDCs treated with 17 μm sized particles did not show any significant upregulation of activation markers by 48 h of treatment. This may be due to a combination of the aforementioned low level of Ag release and low number of particle uptake. We have also previously shown that empty PLGA particles do not upregulate CD86 (10).

These results show that particulated Ag delivery is more effective than soluble Ag delivery but also that the size of the particle plays a major role in the degree of activation of DCs with smaller particles triggering stronger activation.

The Magnitude of Antigen-Specific Cytotoxic T Lymphocytes Generated Following Vaccination is Determined by the Size of Particles Used

Male C57BL/6 mice (n=4) were treated with different sizes of particulated OVA and CpG ODN. Each mouse was primed on day 0 and boosted on day 7 with an intraperitoneal injection of an equivalent dose of 100 μg of OVA and 50 μg of CpG ODN. Peripheral blood lymphocytes from treated mice were stained for frequency of OVA-specific CTL on days 14 and 21. As demonstrated in Fig. 7, mice vaccinated using particles with a median size of 300 nm generated significantly more (p<0.05) OVA-specific CTLs on day 14 as well as on day 21 when compared to all other groups. The frequency of OVA-specific CTLs in all mice vaccinated with particulated groups except for 300 nm sized particles were found to

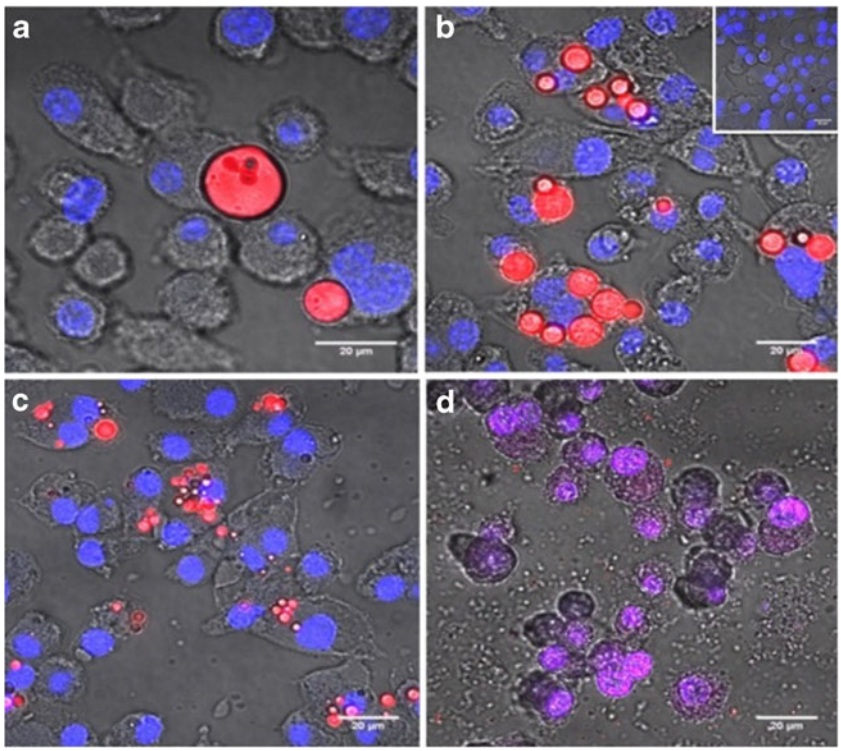

Fig. 4. Internalization of rhodamine B loaded PLGA particles of **a** 17 μm, **b** 7 μm, **c** 1 μm, and **d** 300 nm sizes were studied in JAWS II cells using confocal microscopy. Cells were incubated with particles for 24 h at 37°C. The 17 μm sized particles were not readily internalized by the cells. As the median particle size decreased, more particles were internalized by the JAWS II cells. *Insert* on top right corner represents cells treated with an equivalent dose of soluble rhodamine B. *Scale bar* is 20 μm in length

marginally, but not significantly, increase on day 21 ((ii) in Fig. 7) as compared to day 14 ((i) in Fig. 7). Mice vaccinated with 1 μm sized particles were significantly different from naïve mice ($p<0.05$) on day 21. The low CTL response from mice vaccinated with Ag in solution suggests that quick release from the 300 nm particles is not the dominant factor in the magnitude of the response generated. These results demonstrate that the smaller-sized particles as vaccine

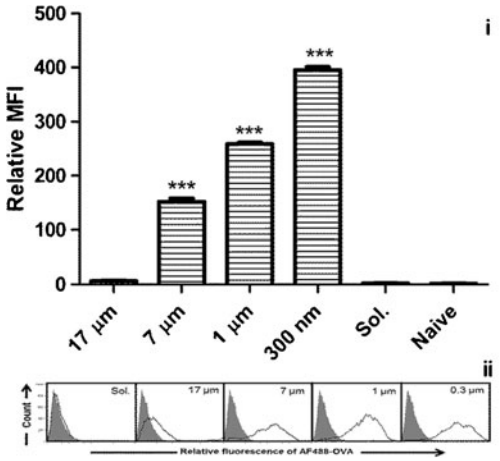

Fig. 5. The efficiency of different sizes of particles to deliver Alexa Fluor 488 conjugated OVA (AF488-OVA) was studied in JAWS II cells using flow cytometry. (*i*) Relative median fluorescent intensity (relative MFI + SEM) of AF488-OVA signal upon incubation of different sizes of particles with JAWS II cells ($n=3$). 7 μm, 1 μm and 300 nm sized particles show significantly higher relative MFI relative to soluble AF488-OVA when compared by ANOVA followed by Tukey's post-test (***$p<0.001$). (*ii*) Representative flow cytometry data showing uptake of AF488-OVA in different treatment groups

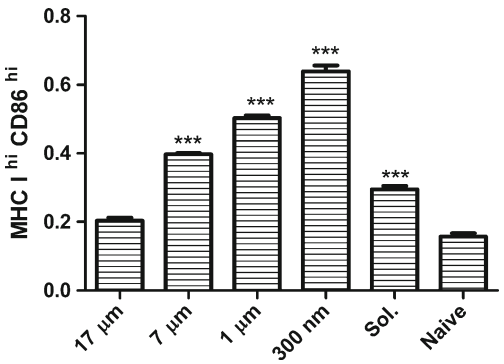

Fig. 6. Upregulation of MHC class I and CD86 expression on BMDCs is dependent on particle size. Flow cytometry analysis representing the fraction of BMDCs with high expression of MHC class I (MHC I hi) and CD86 (CD86 hi) surface molecules. BMDCs were incubated with equivalent amounts of soluble and particulated forms of OVA (4 μg) and CpG ODN (2 μg) for 48 h at 37°C. Experiments were performed in triplicate (mean + SEM). Cells treated with 7 μm, 1 μm, 300 nm sized particles and soluble OVA and CpG ODN showed significantly higher expression of MHC class I and CD86 relative to naïve cells when compared by ANOVA followed by Tukey's post-test (***$p<0.001$)

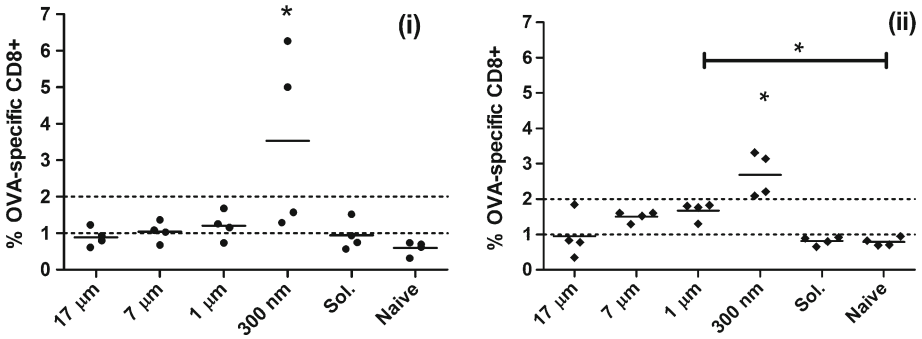

Fig. 7. Analysis of OVA specific T cell frequency in mouse PBLs after delivery of OVA and CpG ODN in different particulate and soluble groups was analyzed by tetramer staining. PBLs were obtained from submandibular bleeding of mice (n=4) vaccinated with OVA (100 µg) and CpG ODN (50 µg) on days 0 and 7. OVA specific T cell frequency was measured on day14 (*i*) and day 21 (*ii*). Mice vaccinated with 300 nm sized particles showed significantly higher OVA specific CD8+ T cells on days14 and 21 relative to naïve mice whereas 1 µm sized particles showed significant difference to naïve mice on day 21 only. All groups were compared using ANOVA followed by Tukey's post-test (*p<0.05)

delivery systems activate significantly higher frequency of CTLs at earlier time points and maintain the level for a prolonged period of time.

IgG2a Levels and IgG2a:IgG1 Ratios are Determined by Size of Particles

Mice were immunized as described in the "MATERIALS AND METHODS" section. Serum IgG antibodies were measured on day 28 using ELISA. Immunization of mice with PLGA particles coloaded with OVA and CpG have been previously shown to induce OVA-specific IgG antibodies (12). Delivery of Ag and adjuvant induces mixed IgG isotype antibody responses that have significant therapeutic activity (2,3). A higher proportion of IgG2a antibodies relative to IgG1 antibodies correlates with secretion of a set of cytokines that favor CTL proliferation (4). Thus, the IgG2a:IgG1 ratio reflects the phenotype of Ag specific responses generated as a result of vaccination (34). Irrespective of size, all particulated groups demonstrated significantly greater levels (p<0.05) of OVA-specific IgG2a antibodies than soluble OVA plus CpG. This highlights the importance of particle-based vaccines and the codelivery of antigens and adjuvants for generation of systemic immunity. However, there were dramatic differences between mice vaccinated with different particle sizes and the OVA-specific IgG2a responses generated. Figure 8(i) shows that the IgG2a antibody responses on day 28 were significantly higher (p<0.05) in mice vaccinated with 300 nm sized PLGA particles relative to all other groups. Mice vaccinated with 300 nm sized particles also gave more than a 50-fold increase in the IgG2a:IgG1 ratio ((ii) in Fig. 8) suggesting polarization of a Th1-type immune response that has been reported to be correlated with therapeutic activity. As the particle size used for vaccination increases, the ratio of IgG2a:IgG1 was found to decrease with 1 µm particles generating approximately equal proportions of IgG2a and IgG1 antibodies on day 28. This is consistent with our data showing that smaller sizes of particles favor the generation and proliferation of Ag specific CTLs.

CONCLUSION

PLGA particles show a size-dependent release of encapsulated molecules. Particle internalization by DCs increases with a decrease in particle size. Confocal microscopy and flow cytometry studies confirmed that particles that

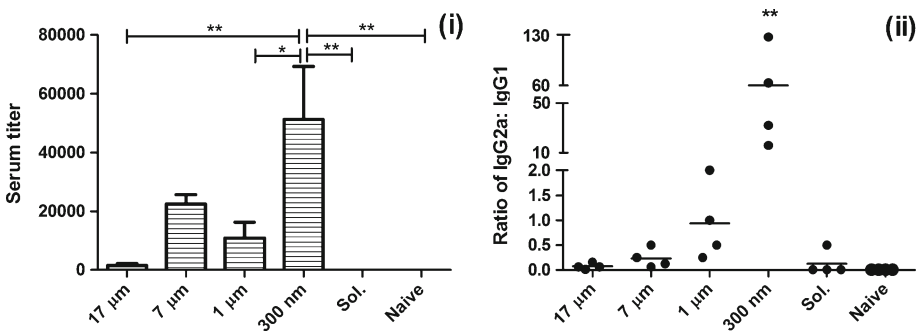

Fig. 8. Anti-OVA IgG antibody levels were measured in mouse serum on day 28. (*i*) The highest dilution of serum displaying OVA specific IgG2a antibody responses as measured by ELISA assay. The bar graph represents mean+SEM of serum titers (n=4). Mice vaccinated with 300 nm sized particles showed significantly higher IgG2a titers when compared to all groups except mice vaccinated with 7 µm sized particles (*p<0.05, **p<0.01). (*ii*) The ratio of IgG2a:IgG1 antibodies in serum samples of different treatment groups on day28. Mice vaccinated with 300 nm sized particles demonstrated the highest ratio of IgG2a:IgG1 antibodies relative to all other groups (**p<0.01)

are 300 nm in size show maximum internalization which when accompanied by its quick release of Ag resulted in maximum activation of BMDCs after 48 h of *in vitro* treatment. The ability to activate BMDCs decreases as the particle size increases.

Mice vaccinated with 300 nm sized particles generated the highest fraction of OVA specific CTLs on days 14 and 21 demonstrating that 300 nm sized particles can rapidly stimulate cell-mediated immunity. This is particularly important in therapeutic treatments of fast growing diseases which are difficult to control at later stages of illness. All particle-based treatment groups generated higher OVA-specific IgG2a antibodies by day 28 relative to soluble antigen. Mice vaccinated with particles that were 300 nm in size generated the highest ratio of IgG2a:IgG1 OVA-specific antibodies by day 28 which was correlated with a relatively higher frequency of OVA specific CTLs measured on days 14 and 21. The smaller the particle size used to vaccinate mice, the greater the magnitude of the Ag-specific CTL response generated.

ACKNOWLEDGMENTS

We gratefully acknowledge support from the American Cancer Society (RSG-09-015-01-CDD) and the National Cancer Institute at the National Institutes of Health (1R21CA128414-01A2/UI Mayo Clinic Lymphoma SPORE). We acknowledge Y. Krishnamachari, Senior Scientist, Merck, Inc. for contributing her expertise to the manuscript. We thank the staff of the Central Microscopy Research Facility, University of Iowa for their assistance with microscopy.

REFERENCES

1. Bremers AJA, Parmiani G. Immunology and immunotherapy of human cancer: present concepts and clinical developments. Crit Rev Oncol Hematol. 2000;34(1):1–25.
2. Weiner GJ, Liu HM, Wooldridge JE, Dahle CE, Krieg AM. Immunostimulatory oligodeoxynucleotides containing the CpG motif are effective as immune adjuvants in tumor antigen immunization. Proc Natl Acad Sci U S A. 1997;94(20):10833–7.
3. Wooldridge JE, Ballas Z, Krieg AM, Weiner GJ. Immunostimulatory oligodeoxynucleotides containing CpG motifs enhance the efficacy of monoclonal antibody therapy of lymphoma. Blood. 1997;89(8):2994–8.
4. Kim JJ, Nottingham LK, Tsai A, Lee DJ, Maguire HC, Oh J, *et al.* Antigen-specific humoral and cellular immune responses can be modulated in rhesus macaques through the use of IFN-γ, IL-12, or IL-18 gene adjuvants. J Med Primatol. 1999;28(4–5):214–23.
5. Gamvrellis A, Leong D, Hanley JC, Xiang SD, Mottram P, Plebanski M. Vaccines that facilitate antigen entry into dendritic cells. Immunol Cell Biol. 2004;82(5):506–16.
6. Waeckerle-Men Y, Groettrup M. PLGA microspheres for improved antigen delivery to dendritic cells as cellular vaccines. Advanced Drug Delivery Reviews. 2005;57(3):475–82.
7. Couvreur P, Vauthier C. Nanotechnology: intelligent design to treat complex disease. Pharm Res. 2006;23(7):1417–50.
8. Elamanchili P, Lutsiak CM, Hamdy S, Diwan M, Samuel J. "Pathogen-mimicking" nanoparticles for vaccine delivery to dendritic cells. J Immunother. 2007;30(4):378–95.
9. Elamanchili P, Diwan M, Cao M, Samuel J. Characterization of poly(D, L-lactic-co-glycolic acid) based nanoparticulate system for enhanced delivery of antigens to dendritic cells. Vaccine. 2004;22(19):2406–12.
10. Zhang XQ, Dahle CE, Baman NK, Rich N, Weiner GJ, Salem AK. Potent antigen-specific immune responses stimulated by codelivery of CpG ODN and antigens in degradable microparticles. J Immunother. 2007;30(5):469–78.
11. Shen H, Ackerman AL, Cody V, Giodini A, Hinson ER, Cresswell P, *et al.* Enhanced and prolonged cross-presentation following endosomal escape of exogenous antigens encapsulated in biodegradable nanoparticles. Immunology. 2006;117(1):78–88.
12. Krishnamachari Y, Salem AK. Innovative strategies for co-delivering antigens and CpG oligonucleotides. Adv Drug Deliv Rev. 2009;61(3):205–17.
13. Ludwig C, Wagner R. Virus-like particles—universal molecular toolboxes. Curr Opin Biotechnol. 2007;18(6):537–45.
14. Coester C, Nayyar P, Samuel J. *In vitro* uptake of gelatin nanoparticles by murine dendritic cells and their intracellular localisation. Eur J Pharm Biopharm. 2006;62(3):306–14.
15. Chikh G, Schutze-Redelmeier MP. Liposomal delivery of CTL epitopes to dendritic cells. Biosci Rep. 2002;22(2):339–53.
16. Torres MP, Wilson-Welder JH, Lopac SK, Phanse Y, Carrillo-Conde B, Ramer-Tait AE, *et al.* Polyanhydride microparticles enhance dendritic cell antigen presentation and activation. Acta Biomater. 2011;7(7):2857–64.
17. Wise DL. Encyclopedic handbook of biomaterials and bioengineering. New York: Marcel Dekker; 1995.
18. Singh M, Briones M, Ott G, O'Hagan D. Cationic microparticles: a potent delivery system for DNA vaccines. Proc Natl Acad Sci U S A. 2000;97(2):811–6.
19. Conway MA, Madrigal-Estebas L, McClean S, Brayden DJ, Mills KH. Protection against *Bordetella pertussis* infection following parenteral or oral immunization with antigens entrapped in biodegradable particles: effect of formulation and route of immunization on induction of Th1 and Th2 cells. Vaccine. 2001;19(15–16):1940–50.
20. Moghimi SM, Porter CJ, Muir IS, Illum L, Davis SS. Non-phagocytic uptake of intravenously injected microspheres in rat spleen: influence of particle size and hydrophilic coating. Biochem Biophys Res Commun. 1991;177(2):861–6.
21. Audran R, Peter K, Dannull J, Men Y, Scandella E, Groettrup M, *et al.* Encapsulation of peptides in biodegradable microspheres prolongs their MHC class-I presentation by dendritic cells and macrophages *in vitro*. Vaccine. 2003;21(11–12):1250–5.
22. Men Y, Thomasin C, Merkle HP, Gander B, Corradin G. A single administration of tetanus toxoid in biodegradable microspheres elicits T cell and antibody responses similar or superior to those obtained with aluminum hydroxide. Vaccine. 1995;13(7):683–9.
23. Peter K, Men Y, Pantaleo G, Gander B, Corradin G. Induction of a cytotoxic T-cell response to HIV-1 proteins with short synthetic peptides and human compatible adjuvants. Vaccine. 2001;19(30):4121–9.
24. Panda AK, Kanchan V. Interactions of antigen-loaded polylactide particles with macrophages and their correlation with the immune response. Biomaterials. 2007;28(35):5344–57.
25. Lavasanifar A, Hamdy S, Molavi O, Ma ZS, Haddadi A, Alshamsan A, *et al.* Co-delivery of cancer-associated antigen and Toll-like receptor 4 ligand in PLGA nanoparticles induces potent CD8(+) T cell-mediated anti-tumor immunity. Vaccine. 2008;26(39):5046–57.
26. Plebanski M, Gamvrellis A, Leong D, Hanley JC, Xiang SD, Mottram P. Vaccines that facilitate antigen entry into dendritic cells. Immunol Cell Biol. 2004;82(5):506–16.
27. Katsikogianni G, Avgoustakis K. Poly(lactide-co-glycolide)-methoxy-poly(ethylene glycol) nanoparticles: drug loading and release properties. J Nanosci Nanotechnol. 2006;6(9–10):3080–6.
28. Tamber H, Johansen P, Merkle HP, Gander B. Formulation aspects of biodegradable polymeric microspheres for antigen delivery. Adv Drug Deliv Rev. 2005;57(3):357–76.
29. Weeratna RD, McCluskie MJ, Xu Y, Davis HL. CpG DNA induces stronger immune responses with less toxicity than other adjuvants. Vaccine. 2000;18(17):1755–62.
30. Yasuda K, Richez C, Uccellini MB, Richards RJ, Bonegio RG, Akira S, *et al.* Requirement for DNA CpG content in TLR9-dependent dendritic cell activation induced by DNA-containing immune complexes. J Immunol. 2009;183(5):3109–17.
31. Krieg AM, Yi AK, Matson S, Waldschmidt TJ, Bishop GA, Teasdale R, *et al.* Cpg motifs in bacterial-DNA trigger direct B-cell activation. Nature. 1995;374(6522):546–9.

32. Lutz MB, Kukutsch N, Ogilvie ALJ, Rößner S, Koch F, Romani N, *et al*. An advanced culture method for generating large quantities of highly pure dendritic cells from mouse bone marrow. J Immunol Methods. 1999;223(1):77–92.
33. Karan D, Krieg AM, Lubaroff DM. Paradoxical enhancement of CD8 T cell-dependent anti-tumor protection despite reduced CD8 T cell responses with addition of a TLR9 agonist to a tumor vaccine. Int J Cancer. 2007;121(7):1520–8.
34. Lee SW, Sung YC. Immuno-stimulatory effects of bacterial-derived plasmids depend on the nature of the antigen in intramuscular DNA inoculations. Immunology. 1998;94 (3):285–9.
35. Prabha S, Zhou WZ, Panyam J, Labhasetwar V. Size-dependency of nanoparticle-mediated gene transfection: studies with fractionated nanoparticles. Int J Pharm. 2002;244(1–2):105–15.
36. Zauner W, Farrow NA, Haines AMR. *In vitro* uptake of polystyrene microspheres: effect of particle size, cell line and cell density. J Control Release. 2001;71(1):39–51.
37. Gil-Torregrosa BC, Lennon-Dumenil AM, Kessler B, Guermonprez P, Ploegh HL, Fruci D, *et al.* Control of cross-presentation during dendritic cell maturation. Eur J Immunol. 2004;34(2):398–407.
38. Schuler G, Schuler-Thurner B, Steinman RM. The use of dendritic cells in cancer immunotherapy. Curr Opin Immunol. 2003;15(2):138–47.